Out of balance: implications of climate change for the ecological stoichiometry of harmful cyanobacteria

van de Waal, D.B.

Chapter 6

Competition for CO_2 between phytoplankton species: theory and experiments

ABSTRACT - Global atmospheric CO_2 levels are rising and will affect many processes in aquatic ecosystems. Resource competition theory has extensively addressed competition for nutrients and light. Yet, competition for inorganic carbon has not been resolved. We developed a model to investigate phytoplankton competition for inorganic carbon. The model describes dynamic changes in carbon dioxide, carbon speciation, light intensity, alkalinity and pH. We tested the model predictions using monoculture and competition experiments in chemostats with a toxic and nontoxic strain of the cyanobacterium *Microcystis aeruginosa*. In monoculture experiments with low CO_2 supply, the increasing cyanobacterial biomass depleted the concentration of dissolved CO_2, leading to a high pH. The toxic strain reduced the CO_2 concentration to lower values and raised pH to higher values than the nontoxic strain. Conversely, the nontoxic strain performed better at low light intensities. As predicted, the toxic strain became dominant in a competition experiment with low CO_2 supply, whereas the nontoxic strain became dominant in a competition experiment with higher CO_2 supply but low light availability. The model captured the observed reversal in competitive dominance, and was also quantitatively in good agreement with the population dynamics during the competition experiments. Our results demonstrate theoretically and experimentally that rising CO_2 levels can alter the community composition and toxicity of harmful algal blooms.

This chapter is based on the manuscript: Dedmer B Van de Waal, Jolanda MH Verspagen, Jan F Finke, Vasiliki Vournazou, W Edwin A Kardinaal, Linda Tonk, Sven Becker, Ellen Van Donk, Petra M Visser, and Jef Huisman. Competition for CO_2 between phytoplankton species: theory and experiments. To be submitted.

6.1 Introduction

Only a century ago, the atmosphere contained ~285 ppm of CO_2. This has risen to the present-day value of 385 ppm, a level far exceeding the natural range of the past 650 000 years. Climate change scenarios predict that atmospheric CO_2 will rise further, to ~750 ppm by the year 2100 (Solomon *et al*. 2007). These changes may affect many processes in aquatic ecosystems (Doney *et al*. 2009; Van de Waal *et al*. 2010). In particular, rising CO_2 concentrations may have implications for competitive interactions between phytoplankton species. Phytoplankton species utilize CO_2 for photosynthesis, and account for almost 50% of the world's carbon fixation (Field *et al*. 1998; Behrenfeld *et al*. 2006). Yet, despite the global significance of these organisms, theory capable of predicting changes in phytoplankton species composition in response to rising CO_2 is still in its infancy.

When CO_2 dissolves in lakes and oceans it reacts with water to form carbonic acid, which dissociates into bicarbonate and a proton. This reduces pH. Hence, rising CO_2 concentrations cause a gradual reduction in the pH of aquatic ecosystems (Orr *et al*. 2005; Riebesell *et al*. 2007; Doney *et al*. 2009). CO_2 uptake by phytoplankton photosynthesis essentially reverses the chemical reaction. CO_2 depletion may lead to high pH values in dense algal blooms (Talling 1976; Ibelings and Maberly 1998; Hansen 2002). In some eutrophic lakes, the pH may even rise to values of > 10 (Maberly 1996). Phytoplankton species differ in their sensitivity to pH (Shapiro 1990; Hansen 2002; Hinga 2002). Changes in pH are therefore likely to cause shifts in phytoplankton species composition (Shapiro 1990; Caraco and Miller 1998; Møgelhøj *et al.* 2006).

Changes in pH also shift the speciation of dissolved inorganic carbon. Dissolved inorganic carbon (DIC) consists predominantly of CO_2 at low pH (pH < 6.5), of bicarbonate at intermediate pH (6.5 < pH < 10.5), and of carbonate at high pH (pH > 10.5). Although phytoplankton species cannot use carbonate as carbon source, many species can take up both CO_2 and bicarbonate (Kaplan and Reinhold 1999; Martin and Tortell 2008). Interestingly, however, major species-specific differences exist in the relative uptake rates of bicarbonate versus CO_2 (e.g., Rost *et al*. 2003; Moroney and Ynalvez 2007; Price *et al.* 2008). This interspecific variability will likely affect the competitive interactions between phytoplankton species (Tortell *et al*. 2002; Rost *et al*. 2008).

Resource competition theory offers an extensive body of theory and experiments describing such resource-consumer interactions (Tilman 1982). Mathematical models have been developed that explicitly link the population dynamics of competing species with the dynamics of the resources that these species are competing for. Experiments can be run to test the theory, providing a check on the validity of the approach or suggesting new directions for research. Competition for nutrients such as nitrogen and phosphorus has been extensively studied in this way, both in theory and experiments (Tilman 1982; Sommer 1985; Grover 1997). Competition for light has also been well investigated (Huisman *et al.* 1999; Stomp *et al*. 2004; Passarge *et al.* 2006). However, with a few notable exceptions

(e.g., Caraco and Miller 1998), resource competition theory has thus far not addressed competition for inorganic carbon. The major challenge here is that competition for inorganic carbon seems conceptually and experimentally more complex than competition for other limiting resources. It involves depletion of the limiting resource (inorganic carbon), a shift in the relative availability of different carbon sources (CO_2 versus bicarbonate), and a shift in associated environmental conditions (pH).

Harmful cyanobacteria often proliferate in eutrophic waters (Reynolds 1987; Huisman *et al.* 2005), and can produce a variety of toxins including microcystins (Carmichael 2001). Some of these cyanobacteria are buoyant and accumulate at the water surface during weak vertical wind mixing, causing dense surface blooms (Walsby *et al*. 1997; Huisman *et al*. 2004; Jöhnk *et al*. 2008). Such dense surface blooms may be accompanied by high toxin concentrations that pose a major threat to birds, mammals and human health (Chorus and Bartram 1999; Carmichael 2001; Paerl and Huisman 2008). Owing to their high photosynthetic activity, dense surface blooms can strip the surface layer from dissolved inorganic carbon leading to carbon limitation (Ibelings and Maberly 1998). In addition, dense surface blooms reduce light availability as a result of substantial self-shading, which can induce light-limited conditions (Huisman *et al*. 1999; Huisman *et al.* 2004). The current rise in atmospheric CO_2 concentrations enriches surface blooms with CO_2. This may shift the competitive interactions within these blooms from competition for inorganic carbon to competition for light.

In this paper, we will develop new competition theory to predict the population dynamics of competition for dissolved inorganic carbon and light. The theory will focus on dynamic changes in carbon chemistry, pH and light conditions during the time course of competition, and how these environmental changes feed back on the competing species. The theory is tested in chemostat experiments, with full control of CO_2 supply, temperature, light, and nutrient conditions. The experiments are carried out with a toxic and nontoxic strain of the freshwater cyanobacterium *Microcystis aeruginosa*, which can cause dense blooms in eutrophic waters (Verspagen *et al.* 2006; Paerl and Huisman 2008). Interestingly, cyanobacterial blooms often consist of mixtures of toxic and nontoxic strains (Kurmayer and Kutzenberger 2003; Kardinaal *et al*. 2007a; Briand *et al.* 2008). A better understanding of the balance between toxic and nontoxic strains will therefore be of major interest in water management. Recently, Kardinaal *et al.* (2007b) showed experimentally that nontoxic strains were better competitors for light when CO_2 was provided in ample supply. Here, we will combine new theory and experiments to investigate whether the competition between toxic and nontoxic strains is affected by changes in CO_2 availability.

6.2 Theory

Model structure - Our model considers several phytoplankton species competing for inorganic carbon and light in a well-mixed water column. The population dynamics of the species depend on the assimilation of carbon dioxide and bicarbonate. Uptake of carbon dioxide induces dynamic changes in pH. These changes in pH, in turn, affect the availability of the different carbon species, which feeds back on phytoplankton growth. In addition, the growing phytoplankton populations cast more shade, reducing light available for photosynthesis. Here, we describe the general structure of the model, while the exact mathematical formulation of the different functions is detailed in Appendix 2.

Population dynamics - We assume that the specific growth rates of the competing species depend on their intracellular carbon content, also known as carbon quota (Droop 1973; Grover 1991). Let n denote the number of phytoplankton species, let X_i denote the population density of phytoplankton species i, and let Q_i denote its carbon quota. The population dynamics of the competing species, and the dynamic changes in their carbon quota, can be summarized by two sets of differential equations:

$$\frac{dX_i}{dt} = \mu_i X_i - DX_i \tag{1}$$

$$\frac{dQ_i}{dt} = u_{CO_2,i} + u_{HCO_3^-,i} - r_i - \mu_i Q_i \tag{2}$$

where i=1,…,n. The first set of equations describes the population densities of the competing species, where μ_i is the specific growth rate of species i and D is the dilution rate (i.e., the turnover rate) of the system. The second set of equations describes the carbon quota of the species, which increase through uptake of carbon dioxide ($u_{CO2,i}$) and bicarbonate ($u_{HCO3,i}$), and decrease through respiration (r_i) and through dilution of the carbon quota by growth. We assume that the uptake rates of carbon dioxide and bicarbonate are increasing but saturating functions of resource availability as in Michaelis-Menten kinetics, and are suppressed when cells become satiated with carbon (Morel 1987; Ducobu *et al*. 1998). Since carbon assimilation requires energy, we further assume that the uptake rates depend on photosynthetic activity.

The model assumes that the cellular carbon assimilated by phytoplankton consists of structural biomass and a transient carbon pool. The relative size of the transient carbon pool, S_i, is defined as:

$$S_i = \frac{Q_i - Q_{MIN,i}}{Q_{MAX,i} - Q_{MIN,i}} \tag{3}$$

where $Q_{MIN,i}$ is the minimum amount of cellular carbon incorporated into the structural biomass of species i, and $Q_{MAX,i}$ is its maximum amount of cellular carbon. The transient carbon pool can be invested to make new structural biomass, which contributes to further

phytoplankton growth. The specific growth rate of a species is therefore determined by the size of its transient carbon pool:

$$\mu_i = \mu_{MAX,i} S_i = \mu_{MAX,i} \left(\frac{Q_i - Q_{MIN,i}}{Q_{MAX,i} - Q_{MIN,i}} \right) \tag{4}$$

where $\mu_{MAX,i}$ is the maximum specific growth rate of species *i*. Our model formulation resembles Droop's (1973) classic growth model. However, we assume that the cellular carbon quota are constrained between $Q_{MIN,i}$ and $Q_{MAX,i}$, as there are physical limits to the amount of carbon that can be stored inside a cell. Hence, the specific growth rate equals zero if the transient carbon pool is exhausted (i.e., $\mu_i = 0$ if $Q_i = Q_{MIN,i}$), and reaches its maximum if cells are satiated with carbon (i.e., $\mu_i = \mu_{MAX,i}$ if $Q_i = Q_{MAX,i}$).

Dissolved inorganic carbon - Carbon dioxide readily dissolves in water, but only a small fraction of the dissolved carbon dioxide reacts with water forming carbonic acid (H_2CO_3). Carbonic acid may subsequently dissociate into bicarbonate and a proton. The reaction from dissolved carbon dioxide to bicarbonate, and vice versa, depends on pH and is relatively slow (Stumm and Morgan 1996). Bicarbonate can dissociate further into carbonate and a proton. This is a much faster process, such that the dissociation of bicarbonate into carbonate and its reverse reaction are essentially in equilibrium with alkalinity and pH (Stumm and Morgan 1996). In addition to these chemical processes, carbon dioxide and bicarbonate are consumed for phytoplankton photosynthesis, and carbon dioxide is released by respiration.

Dissolved carbon dioxide and carbonic acid cannot be distinguished experimentally. Therefore, let $[CO_2]$ denote the total concentration of dissolved carbon dioxide and carbonic acid. In addition, let [CARB] denote the total concentration of bicarbonate and carbonate. Changes in dissolved inorganic carbon can then be described by (Johnson 1982; Stumm and Morgan 1996):

$$\frac{d[\mathrm{CO_2}]}{dt} = D([\mathrm{CO_2}]_{\mathrm{IN}} - [\mathrm{CO_2}]) + g_{CO_2} + c_{CO_2} + \sum_{i=1}^{n} r_i X_i - \sum_{i=1}^{n} u_{CO_2,i} X_i \tag{5}$$

$$\frac{d[\mathrm{CARB}]}{dt} = D([\mathrm{CARB}]_{IN} - [\mathrm{CARB}]) - c_{CO_2} - \sum_{i=1}^{n} u_{HCO_3^-,i} X_i \tag{6}$$

The first equation describes changes in the concentration of dissolved carbon dioxide through the influx ($[CO_2]_{IN}$) and efflux of water containing dissolved CO_2, through gas exchange with atmospheric CO_2 (g_{CO2}), and through the chemical reaction from dissolved CO_2 to bicarbonate and vice versa (c_{CO2}). In addition, the concentration of dissolved carbon dioxide increases through respiration (r_i) and decreases through uptake of CO_2 ($u_{CO2,i}$) by the phytoplankton species. The second equation describes changes in the summed concentration of bicarbonate and carbonate through in- and efflux of water containing these inorganic carbon species, through the chemical reaction from bicarbonate to dissolved CO_2

and vice versa (c_{CO2}), and through uptake of bicarbonate ($u_{HCO3,i}$) by the phytoplankton species. The concentrations of bicarbonate and carbonate are calculated from [CARB] assuming equilibrium with alkalinity and pH (Portielje and Lijklema 1995; Stumm and Morgan 1996).

Alkalinity and pH - Alkalinity is defined as the acid-neutralizing capacity of water. In our experiments, alkalinity is dominated by dissolved inorganic carbon and inorganic phosphates. We note that carbon assimilation by phytoplankton affects pH, but does not change alkalinity. However, nitrate, phosphate and sulfate assimilation are accompanied by proton consumption to maintain charge balance. Assimilation of these nutrients therefore increases alkalinity (Brewer and Goldman 1976; Wolf-Gladrow *et al*. 2007). More specifically, both nitrate and phosphate uptake increase alkalinity by 1 mole equivalent, whereas sulfate uptake increases alkalinity by 2 mole equivalents (Wolf-Gladrow *et al*. 2007). Accordingly, changes in alkalinity can be described as:

$$\frac{d\mathrm{ALK}}{dt} = D\left(ALK_{IN} - ALK\right) + \sum_{i=1}^{n}\left(u_{N,i} + u_{P,i} + 2u_{S,i}\right)X_i \qquad (7)$$

This equation states that changes in alkalinity depend on in- and efflux of water with a given alkalinity, and on the uptake rates of nitrate ($u_{N,i}$), phosphate ($u_{P,i}$), and sulfate ($u_{S,i}$) by the phytoplankton species. At each time step, the pH is calculated iteratively from alkalinity (see Appendix 2).

Light gradient - Light availability determines the photosynthetic rate, and thereby affects the amount of energy available for carbon assimilation. We therefore also monitor the vertical light gradient. According to Lambert-Beer's law, the light intensity penetrating to the bottom of the water column (I_{out}) can be written as (Huisman and Weissing 1994; Huisman *et al.* 1999):

$$I_{out} = I_{in}\exp\left(-K_{bg}z_M - \sum_{i=1}^{n}k_i X_i z_M\right) \qquad (8)$$

This equation states that the light intensity transmitted through the water column increases with the incident light intensity (I_{in}), but decreases with the depth of the water column (z_M), the background turbidity due to light attenuation by water and other non-phytoplankton components (K_{bg}), the specific light attenuation coefficients of the phytoplankton species (k_i), and the population densities of the phytoplankton species.

For a full description of the model, we refer to Appendix 2.

6.3 Methods

Species - The model predictions were tested in a series of monoculture and competition experiments with a toxic and nontoxic strain of the freshwater cyanobacterium *Microcystis aeruginosa* (Kützing) Kützing. Both strains were obtained from the culture collection of the Norwegian Institute for Water Research (NIVA). The toxic strain *Microcystis* CYA140 produces the hepatotoxin microcystin-LR, whereas the nontoxic strain *Microcystis* CYA43 does not produce microcystins. The *Microcystis* strains were grown as single cells, not in colonies. The monoculture experiments were unialgal but not axenic. However, regular microscopic inspection confirmed that population densities of heterotrophic bacteria remained low (i.e., well below 1% of the total biomass).

Chemostat experiments - The experiments were carried out in laboratory-built chemostats specifically designed to study phytoplankton competition (Huisman *et al*. 1999; Stomp *et al.* 2004; Passarge *et al.* 2006). Each chemostat consisted of a flat culture vessel illuminated from one side to obtain a unidirectional light gradient. Light was supplied at a constant incident irradiance of I_{in} = 50 ± 1 µmol photons m^{-2} s^{-1} by white fluorescent tubes (Philips PL-L 24W/840/4P, Philips Lighting). The chemostats had an optical path length ("mixing depth") of z_M = 5 cm, and an effective working volume of 1.7 L. The chemostats were run at a dilution rate of D = 0.011 h^{-1}, and maintained at a constant temperature of 21.5 ± 1 ºC using a metal cooling finger connected to a Colora thermocryostat. The chemostats were supplied with a nutrient-rich mineral medium as described by Van de Waal *et al*. (2009) to prevent nutrient limitation during the experiments. The mineral medium contained 500 µM $NaHCO_3$, and had a pH of ~8.2 in the absence of phytoplankton. The chemostats were aerated with sterilized (0.2 µm Millex-FG Vent Filter, Millipore) and moistened N_2 gas enriched with 200 ppm of CO_2 to a final gas flow of 25 L h^{-1} using Brooks Mass Flow Controllers (Brooks Instrument, Hatfield, PA, USA). We note that the CO_2 concentration in the gas flow is lower than the atmospheric CO_2 level, which might suggest that the applicability of our chemostat experiments is limited. However, the gas flow ensures that the total influx of CO_2 into the chemostat experiments is higher than in natural lakes. Proper up-scaling using model simulations would thus be required to translate these small-scale chemostat experiments to large-scale ecosystems.

Measurements - During the experiments, the chemostats were sampled and several variables were measured every other day until the cultures were in steady state (i.e., with constant population densities and pH) for at least ten days. The incident irradiance (I_{in}) and the irradiance penetrating through the chemostat vessel (I_{out}) were measured with a LI-COR LI-250 quantum photometer (LI-COR Biosciences) at 10 randomly chosen positions on the front and back surface of the chemostat vessel, respectively. Population densities of

Microcystis were determined in triplicate using a Casy 1 TTC cell counter with a 60 µm capillary (Schärfe System GmbH).

Dissolved inorganic carbon (DIC) concentrations in the chemostats were determined by sampling 15 mL of culture suspension, which was immediately filtered over 0.45 µm membrane filters (Whatman). DIC was analyzed by a Model 700 TOC Analyzer (OI Corporation). The concentration of dissolved CO_2 and bicarbonate in the chemostat vessels was calculated from total DIC, pH and temperature (Stumm and Morgan 1996). The pH was measured with a SCHOTT pH meter (SCHOTT AG). Alkalinity was determined in a 50 mL sample that was titrated in 0.1 – 1 mL steps with 0.01 mol L^{-1} HCl to a pH of 3.0. The alkalinity was subsequently calculated using Gran plots according to Stumm and Morgan (1996).

Quantitative polymerase chain reaction - The toxic and nontoxic *Microcystis* strain looked very similar, and could not be distinguished by means of light microscopy, cell counters, or flow cytometry. Therefore, we used the quantitative real-time polymerase chain reaction (Q-PCR) to quantify the population densities of the two strains in the competition experiments. This improves earlier methodology developed by Kardinaal *et al*. (2007b), who distinguished the same two strains with a less precise semi-quantitative method using denaturing gradient gel electrophoresis (DGGE). We measured the relative abundance of microcystin-producing genomes by targeting the *mcyE* region of the microcystin synthetase gene cluster (*mcyE*), which was compared with the 16S rDNA gene (16S). The *mcyE* gene is present only in the toxic strain CYA140, whereas the 16S gene is present in both strains. The *mcyE*:16S ratios were normalized to the inoculation ratio of 0.5, since cells of the two strains were inoculated in a 50:50 ratio at the onset of the competition experiment. Thus, the *mcyE*:16S ratio indicates the relative abundance of the toxic strain in the total *Microcystis* population, where the total *Microcystis* population was counted by the Casy 1 TTC cell counter as described earlier. This yielded the cell number of both strains. Because the used *Microcystis* strains differ in their cell size, and the cell size changes in response to the experimental treatments, we expressed the population densities in biovolume. Biovolumes of the two strains in the competition experiment were estimated using their cell sizes measured in monoculture (Table A3). Because of differences in cell size, the inoculation ratio of the toxic versus nontoxic strain expressed in biovolume was 33:67.

The *mcyE* gene was amplified using the Maeru-mcyEF (5'-ccctagcatcgggttatcat-3') and Maeru-mcyER (5'-cgagtcaattgatattcaatttctc-3') primers (modified from Rantala e*t al*. 2004), and the 16S rDNA gene was amplified using the Maeru-16SrDNAF (5'-gcgtgctactgggctgta-3') and Maeru-16SrDNAR (5'-tcgggtcgatacaagcc-3') primers (modified from Doblin *et al.* 2007).

Aliquots of culture suspension were pressurized at 10 bar to collapse the gas vesicles of *Microcystis* cells, and subsequently centrifuged for 5 minutes at 15 000 *g*. After removal of supernatant, genomic DNA was extracted using a DNeasy® Blood & Tissue Kit

according to the manufacturer's instruction (Qiagen GmbH). The DNA concentration of the samples was measured using a NanoDrop® ND-1000 (Nano-Drop Technologies), and all samples were diluted to an equal density of 10 ng μl^{-1}. The Q-PCR was performed with a Rotor Gene 6000 thermal cycling system (Corbett Research). Each reaction was performed in triplicate. The reaction mix contained 2 µl of sample DNA in combination with 10 µl ABSolute QPCR SYBR green mix (ABgene), 0.3 µl of both the forward and reversed primer of the specific gene tested for, and was filled with 0.1 µm filter sterilized DNase-, RNase-, and Protease-free water (Sigma-Aldrich) to reach a final reaction volume of 20 µl. The thermal cycle consisted of an initial denaturation at 95 °C for 15 min, followed by 40 cycles of denaturation at 94 °C for 20 s, and annealing for 60 s at 65 °C. Data were acquired at 65 °C, and reaction products were verified by DNA melting curve analysis at a temperature ranging from 60 °C to 95 °C at steps of 0.5 °C. Amplification efficiencies of the Q-PCR reactions were comparable in all experiments.

Microcystin analysis - According to expectation, the total microcystin concentration in the competition experiment should vary with the population density of the toxic strain. The performance of the Q-PCR analysis could therefore be assessed independently, by comparison of the estimated population densities of the toxic strain against the microcystin concentrations measured in the culture vessel. Intracellular microcystin content was determined in triplicate by sampling 5-20 mL of culture suspension, which was immediately filtered using Whatman GF/C filters (pore size ~1.2 µm). Filters were frozen at -20°C and subsequently freeze-dried. Microcystins were extracted in three rounds with 75% MeOH according to Fastner *et al*. (1998), with an additional step for grinding of the filters using a Mini Beadbeater (BioSpec Products) with 0.5 mm silica beads (Tonk *et al*. 2005). Dried extracts were stored at -20°C and dissolved in 50% MeOH for microcystin analysis using high performance liquid chromatography (HPLC) with photodiode array detection (Kontron Instruments). The different microcystin variants were separated using a LiChrospher 100 ODS 5 µm LiChorCART 250-4 cartridge system (Merck) and a 30 to 70% acetonitrile gradient in milli-Q water with 0.05% trifluoroacetic acid at a flow rate of 1 mL min^{-1}. Identification of microcystin-LR was based on its characteristic UV-spectra (Lawton *et al*. 1994), and quantified using a gravimetrical standard of microcystin-LR (provided by the University of Dundee). Extracellular microcystin concentrations were determined using an enzyme-linked immunosorbant assay (EnviroLogix). Concentrations of extracellular microcystins comprised less than 2% of the total microcystin concentrations in all chemostat experiments and were therefore considered negligible.

Parameter estimation - The model parameters were estimated from the experiments. For this purpose, it is useful to distinguish between system parameters and species parameters. System parameters are under experimental control, and included the incident light intensity (I_{in}), the mixing depth of the chemostats (z_M), the composition of the mineral medium (i.e.,

$[CO_2]_{IN}$, $[CARB]_{IN}$, ALK_{IN}), the dilution rate (D), and the CO_2 concentration in the gas flow (which features in the function g_{CO2}). The background turbidity (K_{bg}) was determined from measurements of I_{in} and I_{out} in chemostats filled with mineral medium but without phytoplankton. More precisely, according to Lambert-Beer's law (Eq. 8), the background turbidity can be calculated as $K_{bg} = \ln(I_{in}/I_{out})/z_M$. The values of the system parameters are summarized in Appendix 3.

The species parameters were estimated from the monoculture experiments. For this purpose, we fitted the time courses predicted by the model to the time courses of the experimental variables measured in the monoculture experiments. These experimental variables included population density (X_i), total dissolved inorganic carbon, pH, alkalinity, and light penetration through the culture vessel (I_{out}). We followed the same procedure as in earlier studies (Huisman *et al*. 1999; Passarge *et al*. 2006; Agawin *et al*. 2007). Measured data were first log-transformed to homogenize the variances. Subsequently, the log-transformed values were normalized, using the total sum of squares of each experimental variable as weighting factor. Parameter estimates were obtained by fitting the model predictions to these log-transformed normalized data by minimization of the residual sum of squares, using the Gauss-Marquardt-Levenberg algorithm in the software package PEST (Watermark Numerical Computing). The species parameters estimated from the monoculture experiments are summarized in Appendix 3.

Model validation - The parameters estimated from the monoculture experiments were used to predict dynamic changes in population densities, pH, and inorganic carbon concentrations in our competition experiment. In addition, we also compared the model predictions with earlier monoculture and competition experiments by Kardinaal *et al.* (2007b). They studied the same toxic and nontoxic *Microcystis* strains as in our experiments, applying the same chemostat set-up and experimental conditions. However, they used a lower incident light intensity of $I_{in} = 25 \pm 1$ μmol photons m^{-2} s^{-1}, higher CO_2 concentration of 1200 ppm in the gas flow, and higher bicarbonate concentration of 2000 μM $NaHCO_3$ than in our experiments. As a result, their experiments were performed under light-limited conditions, whereas our experiments were performed under CO_2-limited conditions.

6.4 Results

Monoculture experiments - In the monoculture experiments, population densities (expressed as biovolumes) gradually increased until a steady state was reached after 20 to 30 days (Fig. 6.1a,b). Light penetration (I_{out}) through the culture vessels decreased with increasing population density. Steady state values of I_{out} ranged from 5 to 12 µmol photons m^{-2} s^{-1}, which is well above the I_{out} value of 1.3 µmol photons m^{-2} s^{-1} measured for both strains under light-limited but CO_2 replete conditions by Kardinaal *et al.* (2007b). Hence, the steady-state chemostats in our experiments were not light-limited.

As a result of increasing population densities, the carbon chemistry and pH in the water changed (Fig. 6.1c-f). Dissolved CO_2 concentrations were rapidly depleted, showing a more than ten-fold drop to steady-state values of ~0.2 µmol L^{-1} in the monoculture of the toxic strain (Fig. 6.1e) and ~0.6 µmol L^{-1} in the monoculture of the nontoxic strain (Fig. 6.1f). CO_2 depletion was accompanied by an increase of pH to steady-state values of ~10 for the toxic strain and ~9.7 for the nontoxic strain (Fig. 6.1c,d). Interestingly, despite CO_2 depletion, the rise in pH was accompanied by an increase of the total concentration of dissolved inorganic carbon (DIC). Bicarbonate was the predominant carbon species in the water, comprising 68% and 83% of the total DIC in the steady-state monocultures of the toxic and nontoxic strain, respectively. Due to the high pH, about 32% and 17% of the DIC consisted of carbonate, which is not available as carbon source for cyanobacteria.

Model predictions - The model was parameterized based on the monoculture data of the toxic and nontoxic *Microcystis* strain (Fig. 6.1; see for details Appendices 2 and 3). These model parameters allow prediction of the dynamics and outcome of competition for CO_2 and bicarbonate between the two strains. In our case, the predicted winner of competition is not immediately obvious from the parameter estimates. On the one hand, the toxic strain could be favored, because it has higher affinities (i.e., lower half-saturation constants) for CO_2 and bicarbonate and lower minimum carbon quota than the nontoxic strain (Appendix 3). On the other hand, the nontoxic strain could be favored because it has higher maximum uptake rates for CO_2 and bicarbonate. We note, however, that the CO_2 concentration in the monocultures was depleted to lower levels by the toxic strain (Fig. 6.1e,f), which suggests that it might be a better competitor for CO_2.

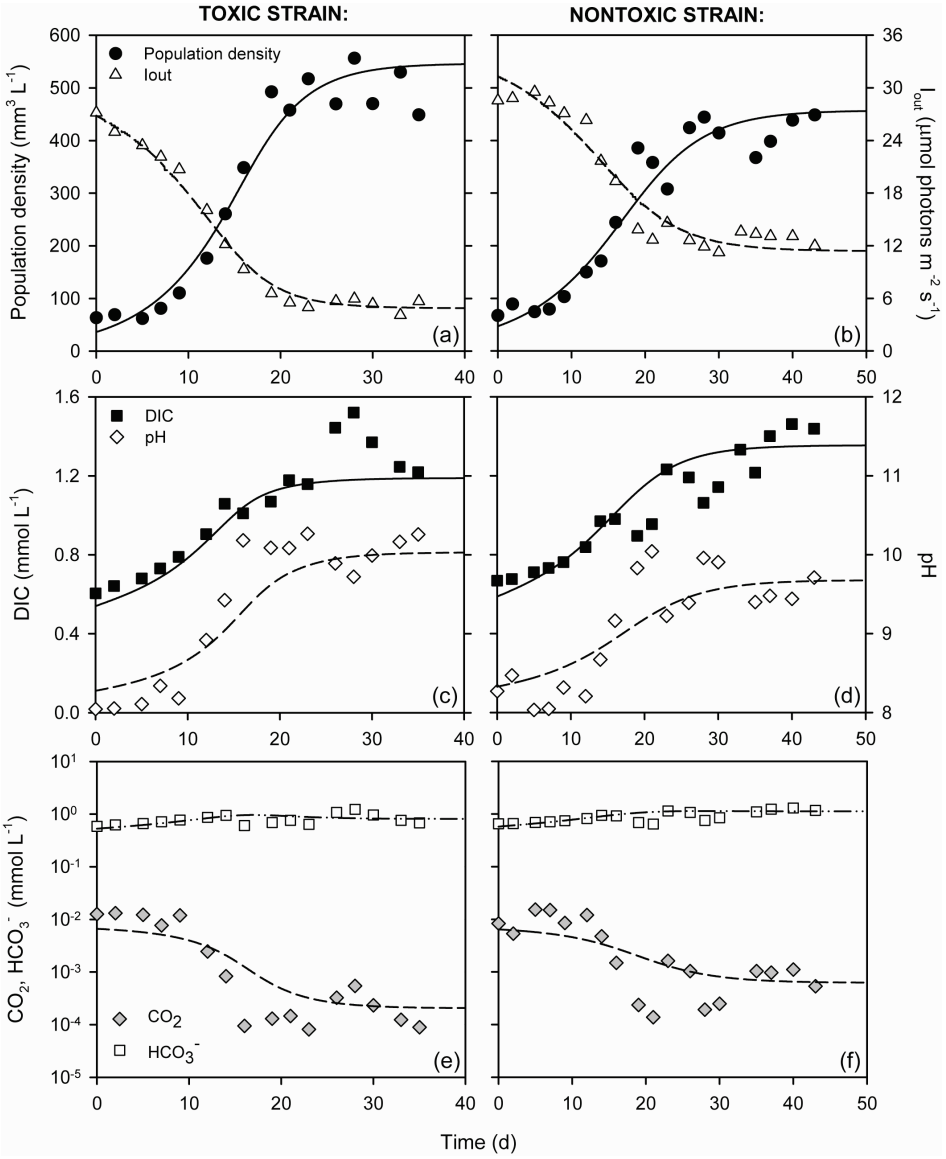

Figure 6.1. Monoculture experiments of the toxic strain *Microcystis* CYA140 and nontoxic strain *Microcystis* CYA43 in CO_2-limited chemostats. (a, b) Population density (expressed as biovolume) and light intensity penetrating through the chemostat (I_{out}), (c, d) dissolved inorganic carbon (DIC) and pH, and (e, f) CO_2 and bicarbonate concentrations. Symbols represent chemostat data, lines show the model fits. Parameter values are provided in Appendix 3.

Resource competition theory has developed a graphical approach using zero isoclines to assess the competitive abilities of species competing for two resources (Tilman 1982). The zero isoclines are plotted in a resource plane, with CO_2 concentrations on the x-axis and

bicarbonate concentrations on the y-axis (Fig. 6.2). At its zero isocline, the net growth rate of a species is zero (i.e., $dX_i/dt=0$). For all combinations of CO_2 and bicarbonate above its zero isocline, a species will increase. For all combinations below its zero isocline, a species will decrease. The species with the lowest zero isocline is the superior competitor; it can survive at lower CO_2 and bicarbonate concentrations than all other species. From our model, we derived an explicit expression to calculate the zero isoclines (Appendix 4). This shows that the zero isoclines of the toxic and nontoxic strain do not intersect. Instead, the toxic strain has the lower zero isocline throughout the resource plane (Fig. 6.2). Thus, the model predicts that the toxic strain will be a better competitor for both CO_2 and bicarbonate than the nontoxic strain.

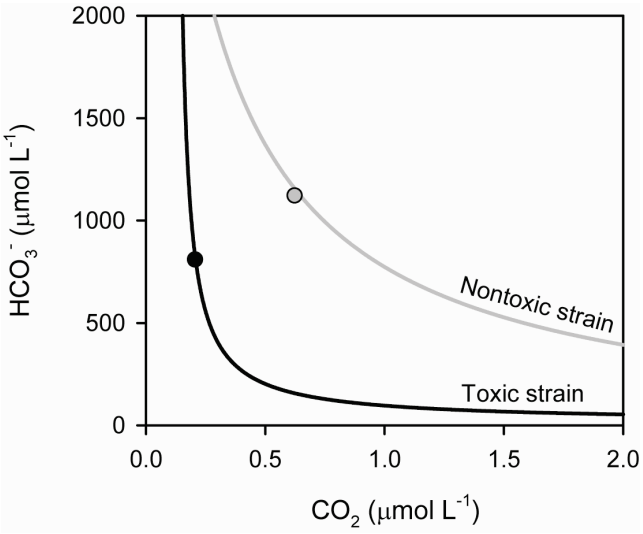

Figure 6.2. Zero isoclines of the toxic strain *Microcystis* CYA140 and nontoxic strain *Microcystis* CYA43 competing for CO_2 and bicarbonate. The zero isoclines are calculated from the model, using the parameter values estimated in the monoculture experiments (see Appendices 3 and 4). Symbols indicate the CO_2 and bicarbonate concentrations measured at steady state in the monoculture of the toxic strain CYA140 (black circle) and the nontoxic strain CYA43 (grey circle).

Competition experiments - The model predictions were tested in competition experiments. In our CO_2-limited competition experiment, population densities of both strains initially increased (Fig. 6.3a). After about 35 days, the dissolved CO_2 concentration was depleted to ~0.2 µmol L^{-1} and pH had increased to ~10 (Fig. 6.3b,c). As a consequence, the nontoxic strain started to decrease and was gradually displaced by the toxic strain (Fig. 6.3a). After 45 days, the nontoxic strain was completely excluded, while the toxic strain approached similar steady-state values as measured in its earlier monoculture experiment.

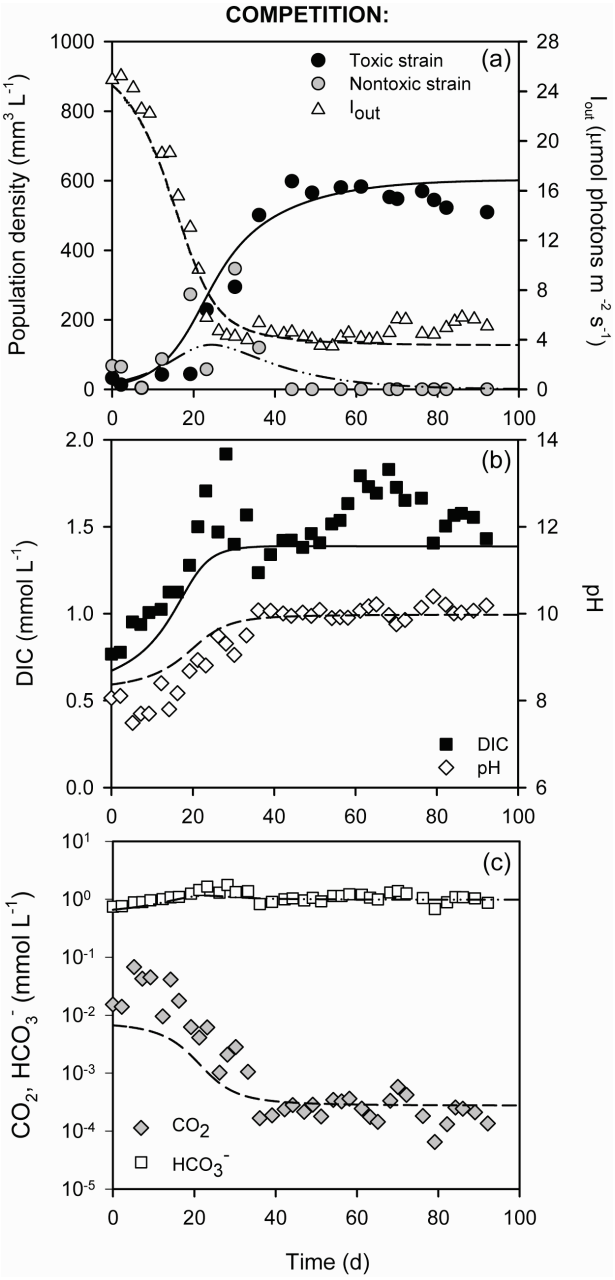

Figure 6.3. Competition between the toxic strain *Microcystis* CYA140 and nontoxic strain *Microcystis* CYA43 in a CO_2-limited chemostat. (a) Population densities of the competing strains (expressed as biovolumes) and light intensity penetrating through the chemostat (I_{out}), (b) dissolved inorganic carbon (DIC) and pH, and (c) CO_2 and bicarbonate concentrations. Symbols represent chemostat data, lines show the model predictions. Parameter values are provided in Appendix 3.

We also tested the model predictions against the monoculture and competition experiments of Kardinaal *et al*. (2007b). Their experiments were performed under light-limited but CO_2-replete conditions. They measured population densities and light availability, but did not measure alkalinity and inorganic carbon concentrations. The monoculture experiments showed that the toxic and nontoxic strain both increased while light penetration through the chemostats (I_{out}) was reduced (Fig. 6.4a,b).

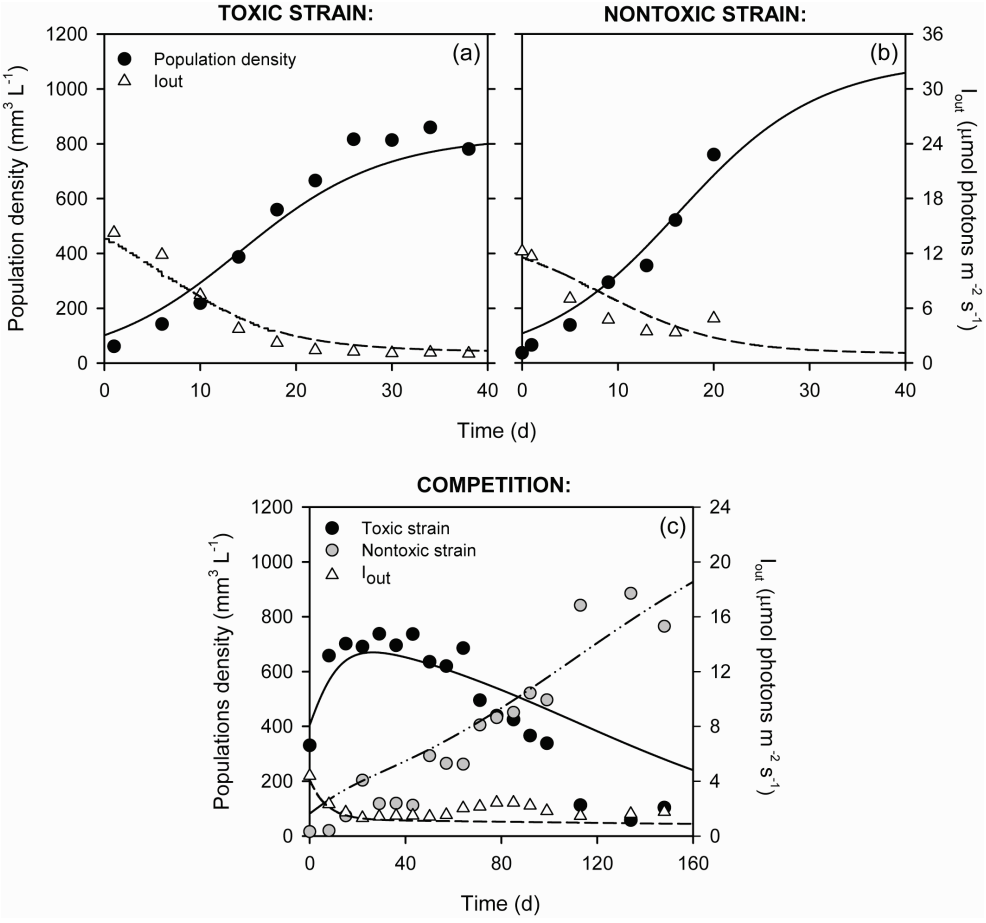

Figure 6.4. Monoculture and competition experiments between the toxic strain *Microcystis* CYA140 and nontoxic strain *Microcystis* CYA43 in light-limited chemostats. (a, b) Population density (expressed as biovolumes) and light intensity penetrating through the chemostat (I_{out}) in the monoculture experiments of (a) the toxic strain *Microcystis* CYA140, and (b) the nontoxic strain *Microcystis* CYA43. (c) Population densities of the two strains (expressed as biovolumes) and light intensity penetrating through the chemostat (I_{out}) in the competition experiment. Symbols represent chemostat data, lines show the model predictions. Parameter values are provided in Appendix 3.

Competition theory predicts that the species that can reduce the light penetration to the lowest level will be the superior competitor for light (Huisman and Weissing 1994; Huisman *et al*. 1999). According to the parameter estimates from our monoculture experiments (Fig. 6.1), the nontoxic strain has a slightly lower half-saturation constant for light and higher maximum uptake rates for inorganic carbon than the toxic strain (Appendix 3). Hence, the model predicts a slightly lower steady-state light penetration of ~1.3 μmol photons m^{-2} s^{-1} for the nontoxic strain, which should make the nontoxic strain a slightly better competitor for light. This model prediction is confirmed by the competition experiment of Kardinaal *et al*. (2007b), where the toxic strain was slowly replaced by the nontoxic strain during a 160-days period (Fig. 6.4c).

In total, the experiments show that the toxic strain becomes dominant under CO_2-limited conditions, while the nontoxic strain dominates under light-limited conditions. The model predictions captured this reversal in competitive dominance, and were also quantitatively in agreement with the experimental results (Figs. 6.3 and 6.4).

Microcystins - The toxic and nontoxic strains of *Microcystis* cannot be distinguished visually under the microscope. Hence, our results rely on molecular techniques estimating the relative abundances of the toxic and nontoxic strains. To confirm the changes in strain composition estimated by the molecular analyses, we measured the changes in microcystin concentration during the competition experiments. In addition, we predicted the changes in microcystin concentration during the competition experiments from model predictions of the abundance of the toxic strain and measurement of its cellular microcystin content. The cellular microcystin content of the toxic strain was 0.52 μg mm^{-3} (s.e. = 0.02; N = 32). The results show good correspondence between observed and predicted microcystin concentrations (Fig. 6.5). In our CO_2-limited competition experiment, the microcystin concentration increased and reached steady state after ~35 days (Fig. 6.5a), confirming the competitive dominance of the toxic strain (Fig. 6.3). Conversely, in the light-limited competition experiment of Kardinaal *et al*. (2007b), the microcystin concentration decreased until the end of the experiment (Fig. 6.5b), consistent with the gradual replacement of the toxic by the nontoxic strain (Fig. 6.4).

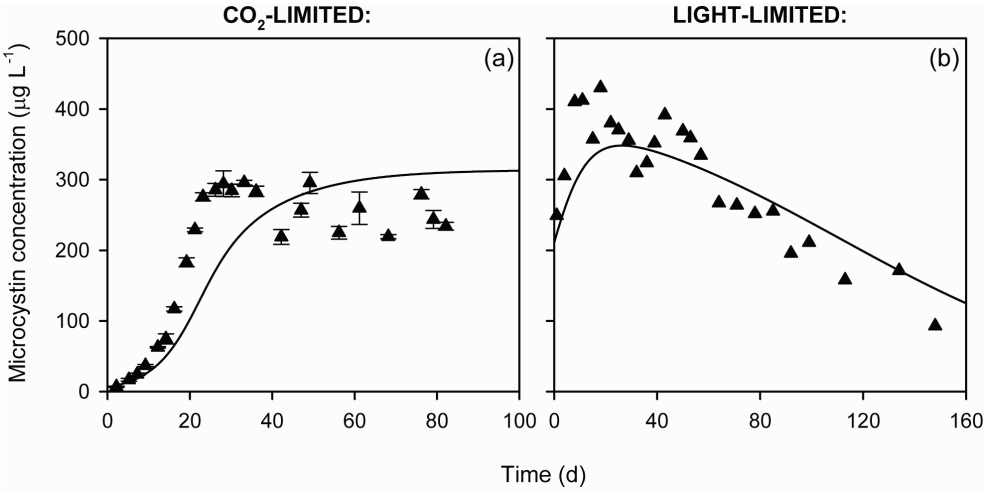

Figure 6.5. Microcystin concentrations in competition experiments between the toxic strain *Microcystis* CYA140 and nontoxic strain *Microcystis* CYA43. Graphs show the total microcystin concentration during (a) competition in the CO_2-limited chemostat and (b) competition in the light-limited chemostat. Error bars indicate SD (n = 3). Symbols represent chemostat data, lines show the model predictions.

6.5 Discussion

Resource competition theory has been extensively studied in laboratory and field experiments with phytoplankton species competing for nutrients (Tilman 1981; Sommer 1985; Grover 1997) and light (Huisman *et al.* 1999; Stomp *et al*. 2004; Passarge *et al.* 2006). However, competition for inorganic carbon has not yet been resolved. A major challenge for studies on competition for inorganic carbon is the strong interplay between CO_2, bicarbonate and pH in aquatic ecosystems. More specifically, as observed in our experiments, carbon assimilation leads to CO_2 depletion accompanied by an increase in pH, shifting the carbon chemistry towards higher bicarbonate concentrations (Fig. 6.1).

The question remains whether CO_2 depletion by the phytoplankton population leads to carbon-limited conditions, since many phytoplankton species can also utilize bicarbonate as additional carbon source (Badger *et al*. 2006). CO_2 easily diffuses across cell membranes. In contrast, utilization of bicarbonate requires active transport mechanisms to cross the cell membrane or the presence of extracellular carbonic anhydrases that convert bicarbonate into carbon dioxide (Kaplan and Reinhold 1999; Elzenga *et al*. 2000; Badger *et al*. 2006). Hence, phytoplankton species typically have a much lower affinity for bicarbonate than for CO_2. This is consistent with our study, where our estimate of the half-saturation constant for bicarbonate was more than two orders of magnitude higher than the estimate of the half-saturation constant for carbon dioxide (Appendix 3). This implies that

cells strongly rely on CO_2 as their preferred carbon source. For instance, our model estimates that 50-60% of the total carbon uptake during the first days of the competition experiment was attributed to CO_2, even though CO_2 concentrations were much lower than bicarbonate concentrations (Fig. 6.3). When CO_2 was depleted and bicarbonate concentrations increased during the course of the competition experiment, the contribution of CO_2 to the total carbon uptake was lower but still amounted to 30% for the toxic strain and 14% for the nontoxic strain. Similar percentages have been reported in other studies (e.g., Rost *et al*. 2003). Thus, the carbon source for phytoplankton growth gradually shifted from combined CO_2 and bicarbonate uptake to predominantly bicarbonate uptake. According to our model simulations, the low uptake rate of bicarbonate was insufficient to sustain the growth rate of the cyanobacteria. Hence, they became carbon limited when CO_2 was depleted.

The zero isoclines of the two strains, deduced from our parameter estimates, indicated that the toxic strain was a better competitor for both CO_2 and bicarbonate (Fig. 6.2). This enabled a straightforward prediction of the outcome of competition for inorganic carbon, i.e., the toxic strain will win. In general, however, it is conceivable that some phytoplankton species are better competitors for CO_2 while other species are better competitors for bicarbonate. If so, this would complicate predictions of the outcome of competition. For instance, it could lead to situations, where CO_2 depletion by the better CO_2 competitors increases bicarbonate availability, which would subsequently facilitate the better competitors for bicarbonate. However, this scenario is beyond the scope of our study, and will require further investigation.

An alternative explanation for the results of our competition experiment is that the pH tolerance differs between the two strains. Indeed, in monoculture, the toxic strain enhanced pH to higher values than the nontoxic strain (Fig. 6.1c,d), and it won the competition experiment. Hence, whereas traditional resource competition models predict the winner of competition based on R* values of competing species, the outcome of our experiments might be explained by differences in pH* values of the two strains. However, preliminary experiments in batch culture indicated that variation in pH had little effect on the specific growth rates of our two strains over the entire pH range covered by our experiments (results not shown). This is consistent with the recent study of Bañares-España *et al*. (2006), who showed that the pH tolerance of 19 different *Microcystis* strains ranged from 10.4 to 11.7, i.e., they could all tolerate high pH. Therefore, our model assumed that pH does not have a direct effect on the specific growth rates (see equation 4). Yet, although *Microcystis* may tolerate high pH, several studies have shown that pH > 9 often approaches or even exceeds the pH tolerance of other phytoplankton species (Goldman *et al*. 1982; Hansen 2002). Further competition experiments with phytoplankton species of different pH sensitivity are therefore recommended to investigate the impact of changes in pH on phytoplankton community composition.

An increase in the CO_2 supply and reduction of the incident light intensity shifted our experiments from competition for inorganic carbon to competition for light. This transition caused a reversal in competitive dominance. The strain dominating under carbon-limited conditions lost the competition under light-limited conditions. This finding seems highly relevant in view of the current rise in atmospheric CO_2 levels, which may alleviate primary producers from carbon limitation. This may particularly apply to dense algal blooms in which inorganic carbon is a potentially important limiting resource. If the reversal in competitive dominance observed in our study is widespread, the next decades may show major changes in the phytoplankton species composition of such algal blooms, from superior carbon competitors to superior light competitors.

In our experiments, the toxic strain was the better competitor for inorganic carbon while the nontoxic strain was the better competitor for light. One might hypothesize that nontoxic strains are generally better competitors for light, because toxin production requires energy, which is less available under light-limiting conditions (Riley and Gordon 1999; Kardinaal *et al*. 2007b). In contrast, carbon-limited conditions may lead to an intracellular excess of light energy and nutrients that can be invested in the production of nitrogen-rich secondary metabolites such as the microcystins. This could favor microcystin-producing strains under carbon-limited conditions, consistent with our experimental results. However, this argument is contradicted by our earlier experiments (Van de Waal *et al*. 2009), where we did not find an increase in microcystin production within a *Microcystis* strain under carbon-limited conditions. Furthermore, the results reported here rely on one toxic and one nontoxic strain only. The observed association between microcystin production and competitive ability of these two strains might be mere coincidence. For instance, differences in competitive ability could be strain specific rather than dependent on the microcystin production of strains. Many more *Microcystis* strains should be studied to elucidate the potential niche requirements of toxic versus nontoxic strains. Irrespective of their microcystin production, our results demonstrate that some *Microcystis* strains are better competitors for inorganic carbon, while other strains are better competitors for light. This implies that environmental variation in carbon and light availability can favor a variety of different strains, which may offer a plausible explanation for the high genetic diversity observed in cyanobacterial blooms (Kurmayer and Kutzenberger 2003; Kardinaal *et al*. 2007a; Briand *et al*. 2008).

In conclusion, our results provide a first step towards a better understanding of competition for inorganic carbon. We have shown that the dynamics and outcome of competition can be predicted from physiological characteristics of the species measured in monoculture. However, our work also raises new questions for future research. For instance, what is the role of pH tolerance in phytoplankton competition for inorganic carbon? And what happens if some species are better competitors for CO_2 while others are better competitors for bicarbonate? To the best of our knowledge, our results provide the first experimental demonstration that changes in the availability of inorganic carbon can

lead to a reversal in the outcome of phytoplankton competition. These results indicate that rising atmospheric CO_2 levels are likely to have major implications for the species composition of algal blooms.

Acknowledgements - The research of DBvdW, JH and PMV was supported by the Earth and Life Sciences Foundation (ALW), and the work of JMHV was supported by the NWO program Water, both subsidized by the Netherlands Organization for Scientific Research (NWO). We thank Prof. Geoff Codd of the University of Dundee for providing the microcystin gravimetrical standards, and Marion Meima for technical support on the Q-PCR.